Photovoltaic Cells Based on GaSb and Ge for Solar and Thermophotovoltaic Applications

V. P. Khvostikov
e-mail: vlkhv@scell.ioffe.rssi.ru

O. A. Khvostikova

P. Y. Gazaryan

S. V. Sorokina

N. S. Potapovich

A. V. Malevskaya

N. A. Kaluzhniy

M. Z. Shvarts

V. M. Andreev

Ioffe Physico-Technical Institute,
26 Polytechnicheskaya,
St. Petersburg 194021,
Russia

In the present work, high efficient photovoltaic (PV) cells based on gallium antimonide have been developed and fabricated with the use of the liquid phase epitaxy (LPE) and diffusion from the gas phase techniques. They are intended for conversion of the infrared (IR) part of the solar spectrum into electricity by tandems of mechanically stacked cells and for conversion of the thermal radiation of emitters heated by the sunlight. On the ground of investigation of the LPE temperature regimes and the tellurium doping effect, GaSb *PV cells have been fabricated with the efficiency of 6% at the concentration of 300 suns behind the single-junction* GaAs *top cell and of 5.6% at the same sunlight concentration of the cells behind the dual-junction* GaInP/GaAs *structure, the substrate thickness being* 100 μm *(the efficiency of PV cells was calculated for AM1.5D Low AOD spectrum,* 1000 W/m^2*). The rated efficiency of conversion of solar powered tungsten emitter radiation by PV cells based on gallium antimonide in a thermophotovoltaic (TPV) module appeared to be about 19%. Photovoltaic cells based on germanium with a wide-gap* GaAs *window grown by LPE or metalorganic chemical vapor deposition and with a p-n junction formed by means of the zinc diffusion from the gas phase have been fabricated. Ge based PV cells without a wide-gap* GaAs *window had the efficiency of up to 8.6% at a concentration of 150 suns. The efficiency of Ge based cells with a wide-gap* GaAs *window was 10.9% at the concentration of 150 suns. 4.3% efficiency Ge cells behind a single-junction* GaAs *top cell at the concentration of 400 suns have been also obtained. The maximum rated conversion efficiency of Ge PV cells appeared to be about 12% in the case of conversion of the tungsten emitter thermal radiation. These efficiency values for Ge based cells are among the highest.* [DOI: 10.1115/1.2734572]

Introduction

Photovoltaic cells based on GaSb may be considered as basic ones at least for two areas of application of the photovoltaic (PV) means for energy production: as narrow-band converters in mechanically stacked tandem solar cells [1–3] and as converters of infrared radiation in thermophotovoltaic systems [3–5].

Usually PV cells based on gallium antimonide are fabricated by means of a relatively simple, as regarding equipment, technological procedure including the diffusion from the gas phase directly into GaSb substrates. It is obvious that the photoconverter output characteristics depend to a large extent on a quality of an initial material, and the epitaxial layers are undoubtedly characterized by a higher morphological perfection compared to a substrates material. The introduction of the epitaxial n-GaSb(Te) base layer with the doping level $n=(2-5)\cdot 10^{17}$ cm^{-3} creates beneficial prerequisites for a better reproducibility of the device parameters, permits us to reduce the background of residual impurities, and to attenuate the effect of the structure inherent point defects. Growth of heavily doped epitaxial layers with a doping level of more than 10^{18} cm^{-3} permits us to obtain a low contact resistance that is necessary to reduce inner ohmic losses in PV cells generating high photocurrent densities. In this work, high efficient photocells based on GaSb intended for conversion of the infrared (IR) part of the solar spectrum by mechanically stacked tandem solar cells and for conversion of radiation from the emitters heated by the concentrated sunlight have been fabricated by liquid phase epitaxy (LPE) and zinc diffusion.

An interest in the investigation of photovoltaic converters based on germanium is dictated, in particular, because at present germanium has become a basic material for fabrication of tandem solar cells either as a substrate material or as a photoactive bottom cell. There also exist resources to raise the efficiency of PV cells based on germanium through increasing the open circuit voltage and the short circuit current. In the present work, the possibilities of using the liquid phase epitaxy or metalorganic chemical vapor deposition (MOCVD) and the gas phase diffusion have been investigated to improve these parameters.

Properties of LPE Grown Gallium Antimonide

The maximum photoluminescence (PL) intensity (Fig. 1) corresponding to the interband charge carrier transitions was observed for epitaxial layers grown by LPE from the gallium melt. The PL peak height for the layers grown with the use of lead solvent was a little bit less than that of the sample obtained from gallium. A noticeable decrease of the PL spectrum intensity was observed for the layers deposited from antimonous melt. Apparently, the type of dominant inherent defects influences the recombination properties of n-GaSb.

Further, growth of gallium antimonide epitaxial layers for PV cells was carried out from the 0.5 mm height melt enriched with gallium. Two regions can be seen on the plot in Fig. 2. In the first one, a rise of the carrier concentration takes place in increasing Te content up to 0.004 at %. An increase of the tellurium concentration in the liquid phase up to 0.006 at % does not result in a noticeable rise of the charge carrier concentration. The theoretical estimation of the dependence shown in Fig. 3 was carried out with the use of the regular solutions model. To calculate the coefficient of the impurity segregation between the solid and liquid phases, the method proposed in Ref. [6] was used. The principle of the approach considers of a semiconductor compound AB doped with

Contributed by the Solar Energy Division of ASME for publication in the JOURNAL OF SOLAR ENERGY ENGINEERING. Manuscript received December 5, 2005; final manuscript received May 12, 2006. Review conducted by Antonio Marti Vega.

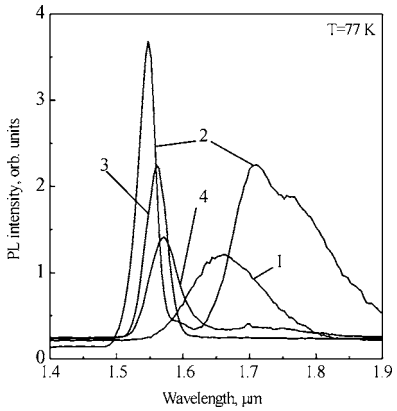

Fig. 1 Photoluminescence spectra of *n*-GaSb (Te) epitaxial layers obtained in different conditions of LPE: (1) substrate material; (2) epitaxy from the melt enriched with Ga; (3) epitaxy from the melt enriched with Pb; and (4) epitaxy from the melt enriched with Sb

an impurity D as a quasi-binary solid solution $AB_{1-x}D_x$, a component of which a "virtual" compound AD contains a doping element.

It is assumed that both compounds (AB and AD) forming the solid solution are isomorphous by the crystalline structure. The heterogeneous equilibrium equation correlating the equilibrium conceptions in the interacting phases can be represented in the form

$$\ln x^s_{AD} \cdot \gamma^s_{AD} = \ln \frac{4x^l_A \cdot x^l_D \cdot \gamma^l_A \cdot \gamma^l_D}{\gamma^{sl}_A \cdot \gamma^{sl}_D} + \frac{\Delta S^F_{AD}}{R \cdot T}(T^F_{AD} - T) \qquad (1)$$

where x^s_{AD} and γ^s_{AD} are the mole fraction and the activity coefficient of a component in the solid phase; x^l_A and γ^l_A are the concentration of components and their activity coefficient in the liquid phase; and ΔS^F_{AD} and T^F_{AD} are the entropy and the temperature of melting of the "virtual" isomorphous compound. In our case, the compound AD means the GaTe compound with the sphalerite structure. According to Ref. [6] this compound is characterized by the following parameters: $T^F = 985$ K and $\Delta S^F \gg 14.7$ cal/mol·K.

According to the regular solutions model for the activity coefficients

$$R \cdot T \cdot \ln \gamma^s_{AD} = \alpha^s \qquad (2)$$

$$R \cdot T \cdot \ln \gamma^l_A = \alpha^l_{AB} \cdot (x^l_B)^2 \qquad (3)$$

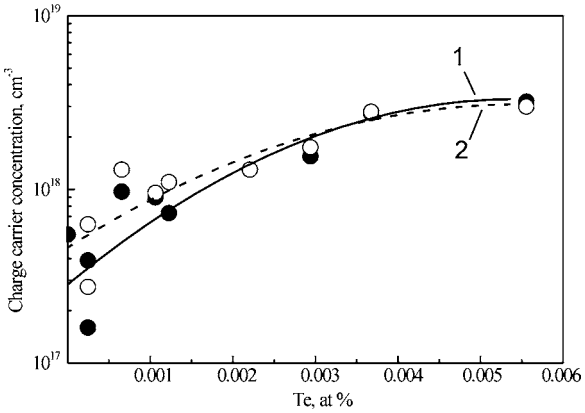

Fig. 2 Dependence of the charge carrier concentration in *n*-GaSb epitaxial layers on the Te atom content in the liquid phase: (1) at 300 K; and (2) at 77 K

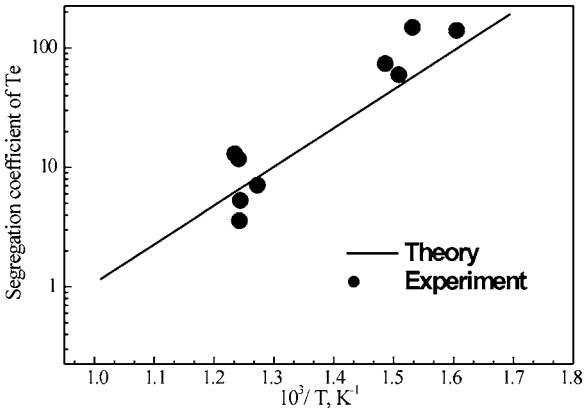

Fig. 3 Segregation coefficient of Te in GaSb as a function of the temperature: theoretical and experimental data

$$R \cdot T \cdot \ln \gamma^l_D = \alpha^l_{AD} \cdot (x^l_A)^2 + \alpha^l_{BD} \cdot (x^l_B)^2 + x^l_A \cdot x^l_B \cdot (\alpha^l_{AD} + \alpha^l_{BD} - \alpha^l_{AB}) \qquad (4)$$

$$R \cdot T \cdot \ln \gamma^{sl}_A = R \cdot T \cdot \ln \gamma^{sl}_D = \alpha^l_{AD}/(4 \cdot R \cdot T) \qquad (5)$$

where α^s, α^{sl}_{mn} are the parameters of the interatomic interaction in the solid and liquid phases, correspondingly; γ^{sl}_A is the activity coefficient of the component in the stoichiometric melt AD.

Taking the impurity distribution coefficient as $K_{Te} = x^s_{Te}/x^l_{Te} = x^s_{GaTe}/2 \cdot x^l_{Te}$, after a number of rearrangements we obtain a formula not explicitly containing the impurity distribution coefficient

$$\begin{aligned} R \cdot T \cdot \ln K_{Te} = {} & \Delta S^F_{GaTe} \cdot (T^F_{GaTe} - T) + R \cdot T \cdot \ln 2 \cdot x^l_{Ga} - \alpha^S \\ & + x^l_{Sb} \cdot \alpha^l_{SbTe} + (x^l_{Ga} - 0.5) \cdot \alpha^l_{GaTe} \\ & + x^l_{Sb} \cdot (x^l_{Sb} - x^l_{Ga}) \cdot \alpha^l_{GaSb} \end{aligned} \qquad (6)$$

The values of the thermodynamical parameters used in the calculations were taken from Ref. [6].

As is seen from Fig. 3, the theoretical dependence fits the experimental data obtained in the present work. It should be noted that at low temperatures of epitaxy a rather high tellurium distribution coefficient (higher than 100) is observed.

Figure 4 shows that the mobility decreases from 4500 $cm^2/V\,s$ to 2500 $cm^2/V\,s$ when the carrier concentration increases from $4 \cdot 10^{17}$ cm^{-3} to $4 \cdot 10^{18}$ cm^{-3}. This fact can be explained by the effect of the charge carrier scattering by ionized impurity atoms, since the majority of the impurity atoms are ionized at room tem-

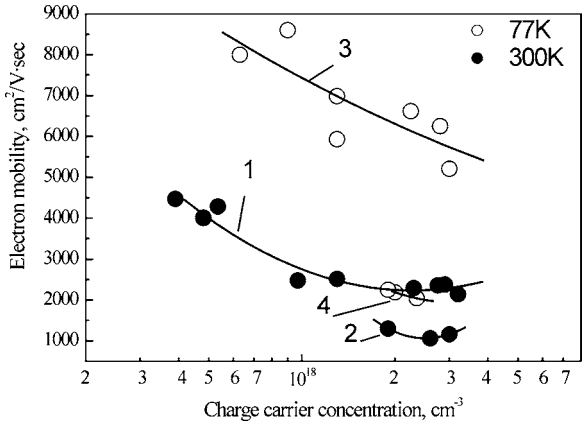

Fig. 4 Dependence of the charge carrier mobility on their concentration in the *n*-GaSb epitaxial layers at 300 K and 77 K at the epitaxy temperatures of 520°C (curves 1, 3) and of 400°C (curves 2, 4)

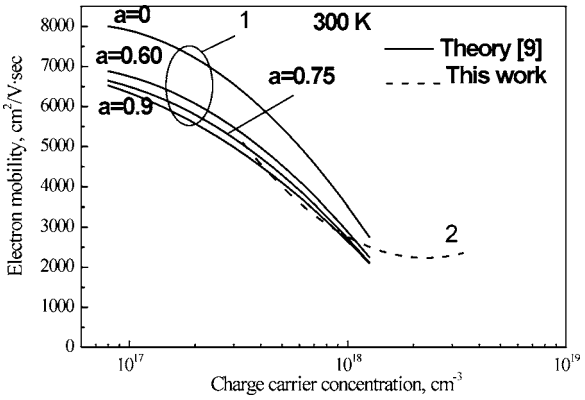

Fig. 5 Dependence of the theoretical (curves 1) and experimental (curve 2) charge carrier mobility on their concentration in the epitaxial (LPE) *n*-GaSb layers at the different compensation coefficient values from *a*=0 to *a*=0.9

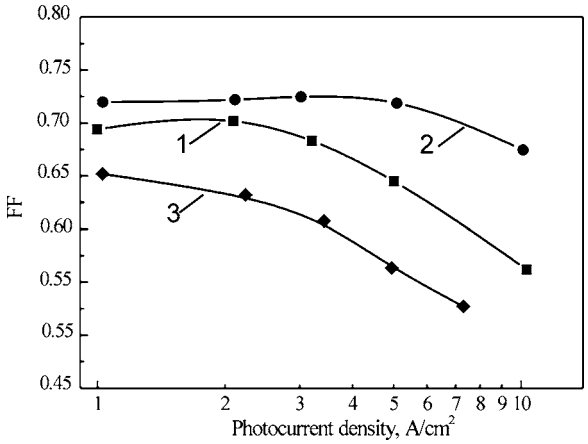

Fig. 6 Dependence of FF on the photocurrent density: (curve 1) the first type cell (GaSb substrate with the doping level $n=(2-6)\cdot10^{17}$ cm^{-3}, the rear n^+ layer); (curve 2) the second type cell (GaSb epitaxial layer on a heavily doped n^+-GaSb substrate); and (curve 3) the third type cell (GaSb substrate with the doping level $n=(2-6)\cdot10^{17}$ cm^{-3})

perature. The epitaxial layers with the charge carrier concentration $n=(3-5)\cdot10^{17}$ cm^{-3} were characterized by the mobilities of >4000 cm^2/V s at 300 K and >8000 cm^2/V s at $T=77$ K. The epitaxial layers with the doping level in the range of $n=(3-6)\cdot10^{17}$ cm^{-3} were intended to create a photosensitive region of PV converters based on gallium antimonide. At a higher doping level in *n*-GaSb, defects appear in the material, which result in the rise of the leakage currents in the *p-n*-junction region that affect the separation of generated charge carriers.

The heavily doped n^+ layers of gallium antimonide ($\geq10^{18}$ cm^{-3}) were grown on the structure rear surface to reduce ohmic contact resistance to about 10^{-6} Ω cm^2 [7]. Such layers can also be used for fabrication of the tunnel *p/n* junctions in monolithic dual-junction photoconverters. It follows from the dependences presented in Fig. 4 that the epitaxial layer growth temperature has an influence on the electron mobility value. For instance, for the layers grown at a temperature of about 400°C, charge carrier mobilities are much lower, compared to those in the layers grown at about 520°C.

As follows from the dependences of the charge carrier mobilities on their concentration in gallium antimonide ingots grown by the Czochralski technique [8], the charge carriers mobility values in the ingot material are lower than those in the epitaxial layers (Fig. 4) for charge carrier concentrations of $5\cdot10^{17}$ cm^{-3}. Thus, the epitaxial growth allows us to obtain layers with high charge carrier mobility values, which may be explained by a smaller amount of defects in the grown layers compared with that in the "bulk" material.

Much attention is given in the literature to the theoretical analysis of the charge carrier mobilities in semiconductors [9–11]. Often in estimating mobilities in these works the effect of a great number of physical parameters, such as scattering by ionized impurities by acoustic phonons etc., is taken into account. However, in the case of the semiconductor compounds, for example gallium antimonide, some of these parameters have not been precisely determined. For this reason, these theories allow us to approximately estimate the limiting values of the mobility of charge carriers in gallium antimonide in relation to their concentration. The model proposed in Ref. [9] was used in calculations of the dependences in Fig. 5, in which $a=N_A/N_D$ (N_A and N_D are the acceptor and donor doping concentrations, correspondingly). It allows estimating the theoretical limit of the charge carrier mobility at different doping levels in *n*-GaSb and for different compensation coefficients. As is seen from Fig. 5, the theoretical limit for the electron mobility is higher than the values obtained from experimental investigations, in particular at low concentrations ($<10^{17}$ cm^{-3}). The experimental data from this work (dash curves 2) are close to the data obtained in Ref. [9] and correspond to the compensation level $a=0.6$ and higher. This comparison allows us to judge the high quality of the grown gallium antimonide layers, which gives the possibility of using these layers for fabrication of high effective PV converters.

PV Converters Based on GaSb

PV cells based on GaSb were fabricated by the combined techniques: LPE and zinc diffusion. As previously shown optimum conditions of the LPE were used for GaSb growth from the melt enriched with gallium. Formation of a *p-n* junction on a light sensitive structure surface and in subcontact areas was carried out by means of the two-stage diffusion [12]. Pure zinc served as a diffusion source. A quasi-closed graphite boat and multideck packing of sliders were used as a process volume [12,13]. The boat was placed into a quartz reactor of the flow type. To prevent oxidation of substrates the diffusion was carried out in a flow of hydrogen purified by a palladium filter. The temperature range of the diffusion was about 450–470°C. The diffusant and the substrate had the same temperature. In a number of cases, pure antimony was added into a boat. To make the ohmic rear contact to GaSb cells, Au(Ge)/Ni/Au was used, and for the front one—Cr/Au and Ti/Pt/Au.

Three types of GaSb PV cells have been developed. The first type—by diffusion into the GaSb substrate with a rear n^+ layer with the substrate doping level $n=(2-6)\cdot10^{17}$ cm^{-3}. The second type—by diffusion into the *n*-GaSb front epitaxial layer without a rear n^+ layer and with the substrate doping level $n=10^{18}$ cm^{-3}. The third type—with diffusion into the GaSb substrate with the doping level $n=(2-6)\cdot10^{17}$ cm^{-3} without a rear epitaxial n^+ layer. Anti-reflection coating (ZnS/MgF_2), contact metallization materials, and grid geometry were the same for all types of cells.

As follows from the dependences presented in Fig. 6, the PV cells with an epitaxial layer grown on a heavily doped substrate (of the second type, curve 2) are characterized by the highest fill factor FF=0.72, which does not decrease with the increase of generated photocurrent densities up to 5 A/cm^2.

As is seen from Fig. 7, the cells with a rear n^+ layer (curve 1) and with an epitaxial layer grown on a heavily doped substrate (curve 2) have a higher value of the efficiency (6%) compared to those of the cells fabricated by zinc diffusion into the GaSb substrate (curve 3). A drop of the efficiency is observed for the cells of the first and third types at the current densities higher than

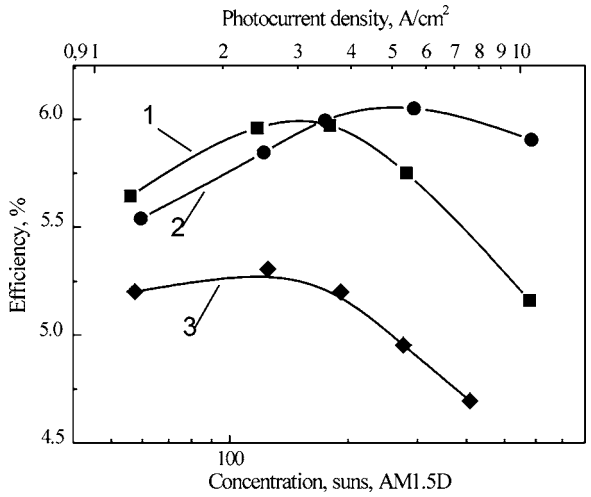

Fig. 7 Dependence of the efficiency for a PV cell based on GaSb behind the top cell based on GaAs on the sunlight illumination density: (curve 1) the first type cell (GaSb substrate with the doping level $n=(2-6)\cdot10^{17}$ cm^{-3}, the rear n^+ layer); curve 2-the second type cell (epitaxial GaSb layer on a heavily doped n^+-GaSb substrate); and (curve 3) the third type cell (GaSb substrate with the doping level $n=(2-6)\cdot10^{17}$ cm^{-3})

3 A/cm^2, but it continues to rise for the cells of the second type (Fig. 7, curve 2). This fact may be explained by the lower ohmic losses at higher current densities in the PV cells on GaSb substrates with the higher doping level ($n=10^{18}$ cm^{-3}).

A GaSb cell has to have a good photosensitivity in the wavelength range of 900–1850 nm when it is used in a tandem mechanically stacked solar cell for conversion of the infrared (IR) radiation passed through the structure of the top cells based on an IR transparent GaAs substrate. Application of the epitaxial technology for the fabrication of GaSb cells together with the optimization of the anti-reflection coating allows for gaining the higher values of the external quantum yield in the spectral range of 1200–1850 nm (Fig. 8). To obtain high values of the photocurrent densities it is also necessary to optimize the top cell construction with the aim to reduce the optical losses of the radiation in the IR spectral range. For this purpose, the top cell substrate thickness was gradually decreased. The photocurrent density of the bottom

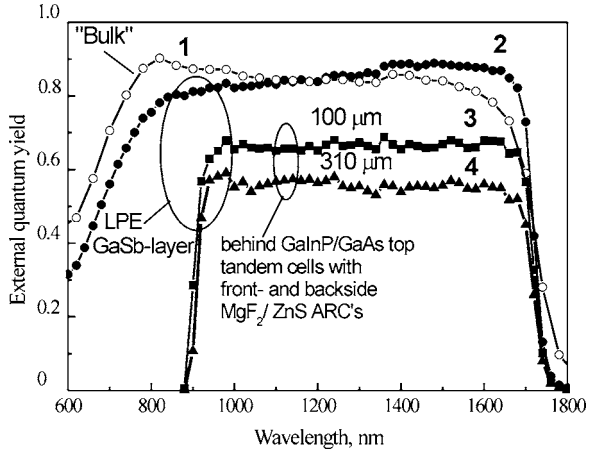

Fig. 8 Spectral responses of GaSb solar cells based on "bulk" (curve 1) and LPE grown (curve 2, 3, 4) photoactive layer as it is (curve 1, 2) and under the top IR transparent GaInP/GaAs cells with GaAs substrate thickness: 100 μm (curve 3) and 310 μm (curve 4)

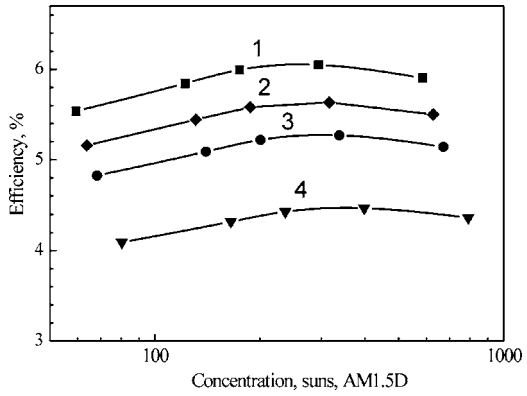

Fig. 9 Efficiency versus sunlight concentration for a GaSb bottom cell illuminated through: (1) GaAs cell based on substrate of 450 μm thick; (2) GaInP/GaAs dual-junction cell based on GaAs substrate of 100 μm thick; (3, 4) GaInP/GaInAs dual-junction cells based on GaAs substrate 250 μm and 410 μm thick, correspondingly. Efficiencies of 6.05% (curve 1) and of 5.6% (curve 2) at 300 suns were achieved

GaSb solar cell increased steadily up to 15.9 mA/cm^2 at the AM1.5 illumination through the top tandem GaInP/GaInAs structure with the substrate thickness of 310 μm and up to 16.6 mA/cm^2 in the case of a top of GaInP/GaAs tandem structure with 100 μm substrate. The improved optical transmittance of the top cell and the use of the epitaxial technology for the bottom cell allows reaching theGaSb cell efficiency of 5.6% (300 suns) (Fig. 9). Further increase of the bottom GaSb cell efficiency is possible by the use of a prismatic cover slide of the top and bottom cells, which reduces the optical losses associated with cell surface shadowing by a contact grid.

With the aim to investigate the possibility of using GaSb cells in solar TPV converters, two designs of the solar TPV modules (of conical and cylindrical types) have been developed and fabricated [14]. The preliminary sunlight concentration was performed by a square Fresnel lens of 0.36 m^2 area ($F=70$ cm) or by a pseudo-parabolic mirror of 0.45 m^2 area with a focus distance of 75 cm. The emitter was made of tungsten or tantalum and was placed either in vacuum, or in an inert gas atmosphere such as argon or xenon. At the use of the secondary quartz lens located above the emitter, the sunlight density incident on the emitter input aperture of 12 mm diameter in St. Petersburg in the summer period was 220–270 W. The maximum short circuit photocurrent density $J_{sc}=4.5$ A/cm^2 has been obtained for a GaSb PV cell under illumination from a tungsten emitter in the conical type system, where the open circuit voltage was $V_{oc}=0.49$ V and the FF $=0.68$.

PV Cells Based on Germanium

To fabricate photovoltaic converters based on germanium, diffusion from the gas phase technique has been chosen. To form an n-type emitter in a p-Ge substrate, antimony, phosphorus, and arsenic can be used. As is known, in doping with phosphorus and arsenic as diffusants the toxic compounds of these elements are often used. Antimony creates a shallow donor level (0.01 eV) in the germanium forbidden gap and has a comparatively large diffusion coefficient. For these reasons, antimony has been chosen as a donor diffusant. The diffusion temperature was 600°C. At higher temperatures, a change of the Ge substrate surface morphology was observed that subsequently resulted in the essential drop of the photocurrent.

To fabricate a p-type emitter in an n-type germanium substrate, the following diffusants can be considered: boron, gallium, indium, zinc, and cadmium. Comparison of the diffusion coefficients of these impurities in germanium [15] shows that boron,

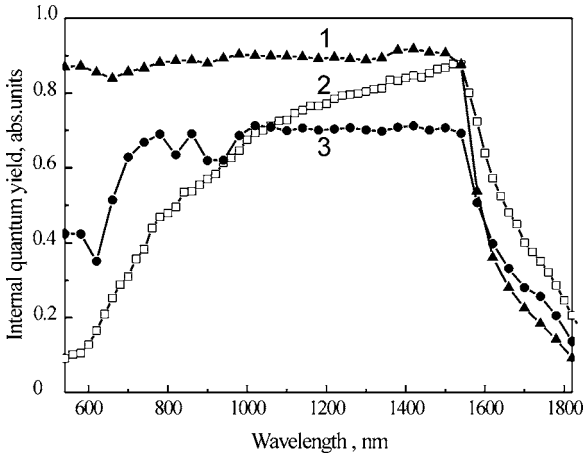

Fig. 10 Internal quantum yield of germanium *n-p* (2) and *p-n* (1, 3) photocells obtained with the use of different diffusants: zinc (1), antimony (2), and boron (3)

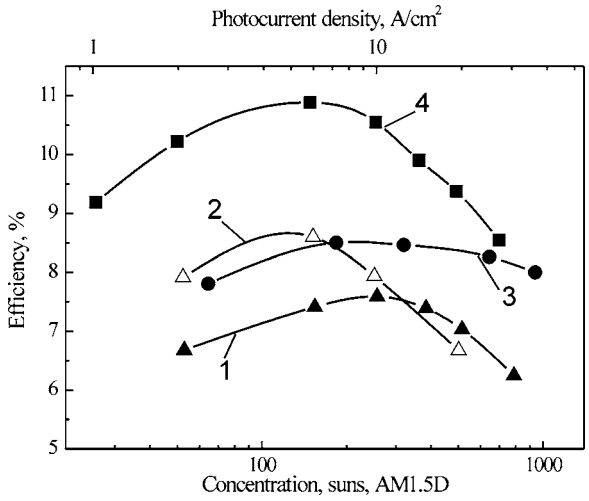

Fig. 11 Dependence of the efficiency of the PV cells based on Ge fabricated by different techniques on the sunlight concentration ratio (AM1.5D spectrum cut off at 1820 nm) and on the short circuit photocurrent density: (1, 2) PV cells based on the *p*-Ge/*n*-Ge structure; (3) PV cells based on the *p*-GaAs/*p*-Ge/*n*-Ge structure with a GaAs window grown by LPE; and (4) PV cells based on the *p*-GaAs/*p*-Ge/*n*-Ge structure with a GaAs window grown by MOCVD

gallium, and indium have diffusion coefficients in the temperature range of 600–750°C by order of magnitude lower than that of zinc. Cadmium cannot be chosen as a doping impurity, originating from a deep acceptor level in the germanium forbidden gap (0.16 eV). Zinc has been chosen as a main acceptor impurity, since it forms a rather shallow acceptor level (0.09 eV); it creates a necessary vapor pressure at a comparatively low diffusion temperature. The zinc diffusion coefficient is $(2-3)\cdot 10^{-14}$ cm^2/s [16] at the chosen diffusion temperature of 680°C.

The possibility of using boron as a diffusant was also investigated since, in spite of its smallest diffusion coefficient compared to that of considered impurities, its undoubtful advantage is formation of a shallow acceptor level in the germanium forbidden gap (0.01 eV). A suitable source for the boron diffusion is diboran (B_2H_6). It can be used in the reducing and neutral medium—in the flows of argon, nitrogen, or hydrogen. At temperature higher than 300°C the diboran pyrolisis takes place with production of elemental boron. In our case the diffusion was carried out at $T=750$°C, at which the boron diffusion coefficient increases to $D=(5-8)\cdot 10^{-14}$ cm^2/s [15].

The photocurrent density (J_{ph}) in *n-p*-Ge photocells fabricated by antimony diffusion into a *p*-Ge(Ga) substrate in the spectral range of 580–1820 nm was 28.1 mA/cm^2 (AM1.5D), in the case of diffusion of boron into an *n*-Ge(Sb) substrate J_{ph} was 30.9 mA/cm^2, and in the case of zinc diffusion J_{ph} reached 41.4 mA/cm^2. It follows from a comparison of the spectral characteristics (see Fig. 10) of the photocells that the maximum photosensitivity is observed for the photocells fabricated by zinc diffusion into *n*-Ge. The short circuit current densities in this case in the wavelength range of 340–1820 nm calculated from the external quantum yield data were 42.3 mA/cm^2 for the AM1.5D spectrum and 53.6 mA/cm^2 for the AM0 spectrum.

For comparison, the average value of the photocurrent density of the GaSb cell considered above is about 37–38 mA/cm^2 in the spectral range of 580–1820 nm for the AM1.5D spectrum and 45 mA/cm^2 in the same spectral range for the AM0 spectrum.

Hence, it follows that germanium cells can have a higher photocurrent than GaSb cells. However, comparison of the electrical characteristics of the Ge and GaSb photocells shows that the weak point of the cells based on Ge is the lower value of the open circuit voltage.

The key means for improving the Ge cells is passivation of the germanium surface. A number of possible passivating films for germanium were developed. They are, for example, SiN_x [16], germanium oxide [17], amorphous silicon [18], GaAs [19], and GaInP [20,21]. As a result of passivation of the germanium surface by silicon nitride [16], an increase of the short circuit current density from 29.4 mA/cm^2 to 52.8 mA/cm^2, of the open circuit voltage from 0.143 V to 0.197 V, of the *I–V* characteristic FF from 48.7% to 57.8% and the efficiency from 2% to 6% for the AM1.5G spectrum have been reported. The authors of Ref. [17] have developed a stable process of a room temperature wet chemical growth of their own oxide layers on germanium cells fabricated by the diffusion technique. The open circuit voltage of 0.24 V and the short circuit current density of 55.5 mA/cm^2 were measured in these cells under the AM0 spectrum. The investigations of the effect of the wide-band GaInPwindow layer (grown by the MOVPE technique) were carried out [20]. It has been shown that after passivation of Ge cells by a wide-band window layer a rise of both the open circuit voltage from 0.17 V to 0.24 V and the *I–V* characteristic FF from 60% to 67.3% at $J_{sc}=16$ mA/cm^2 has been observed.

In the present work, a thin GaAs window layer was used for passivation of the Ge surface. A low-temperature (380°C) LPE technique for growing the GaAs layers has been developed. The growth takes place from a melt enriched with lead at relatively fast cooling rate (2°C/s) over (111) oriented Ge wafer. The *p*-GaAs/*p*-Ge/*n*-Ge PV cell structures have been grown as well using the MOCVD technique at the growth temperature reduced down to 590°C [22].

Figure 11 presents the efficiencies of fabricated 2.5 mm^2 $\times$2.5 mm^2 PV cells based on Ge intended for conversion of concentrated sunlight. PV cells with a wide-band window grown by the LPE technique (curve 3) were fabricated on germanium substrates (111) precisely oriented and doped with antimony, $n=(1-2)\cdot 10^{17}$ cm^{-3}. Curve 1 is related to the cells obtained on a similar substrate, but without a GaAs window. The PV cells with a wide-band window grown by the MOCVD technique (curve 4) were obtained on germanium substrates with the (100) surface orientation 6 deg off to (111) and doped with arsenic, $n=8\cdot 10^{17}$ cm^{-3}. The *p-n* junction in all types of structures was formed by the zinc diffusion from the gas phase. Anti-reflection coating (ZnS/MgF_2), contact metallization materials, and grid geometry were the same for all types of developed cells based on germanium. As follows from the presented dependencies, the

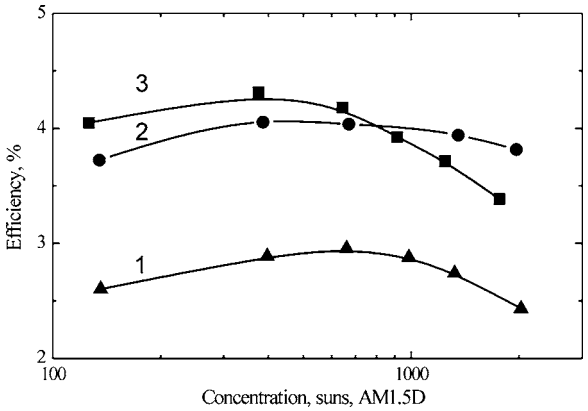

Fig. 12 Dependence of the efficiency of the PV cells based on Ge behind a IR transparent cell based on GaAs (the GaAs substrate thickness was 450 μm) on the sunlight concentration ratio: (1) cells based on Ge ($n\sim10^{17}$ cm^{-3}); (2) cells based on Ge with a LPE grown GaAs window; and (3) cells based on Ge with a MOCVD grown GaAs window

highest conversion efficiencies are 10.9% in the Ge based cell with a GaAs window grown by the MOCVD technique at the concentration ratio of about 150 suns and 8.6% in the germanium cells without GaAs layer obtained on a similar substrate for the same sunlight concentration.

Figure 12 shows the efficiencies of PV cells based on Ge located behind a single-junction cell based on GaAs (the substrate thickness was 450 μm) intended for conversion of the high concentration of the sunlight (up to 2000 suns). It is seen that for concentration lower than 800 suns, the cells with wide-band gap windows grown by MOCVD are the most effective (with maximum efficiency of 4.3% at 400 suns), and for the concentrations from 800 to 2000 suns, the PV cells with window layers grown by LPE are the most effective (with maximum efficiency of 4% at 1000 suns). As it is clear from Fig. 13, an essential increase ($\sim$0.1 V) of the open circuit voltage value was achieved after passivation of the germanium surface with a GaAs window layer.

Comparison of GaSb and Ge Based TPV Cells

The rated efficiency values are 18.5% for GaSb TPV cells and 11.5% for Ge cells at the emitter temperature of up to 2000 K (Fig. 14). In the case of the sub-band gap photon energy return at the use of a rear mirror, the efficiency increases up to 20.5% for GaSb cell at return efficiency RE=50% and 16% for Ge cell at RE=90% (Fig. 15).

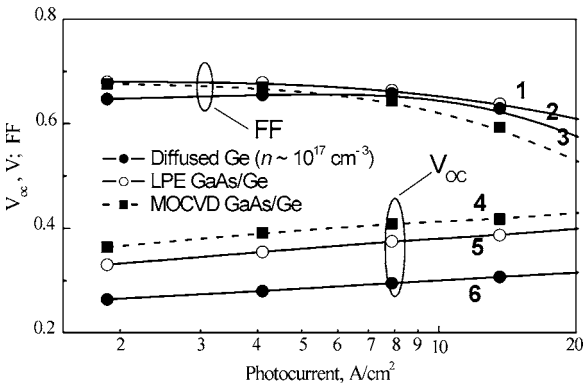

Fig. 13 Dependence of FF (curves 1, 2, 3) and V_{oc} (curves 4, 5, 6) on the photocurrent density for the PV cells based on *p-n*-Ge with (curves 1, 3) and without a GaAs window (curves 2, 6)

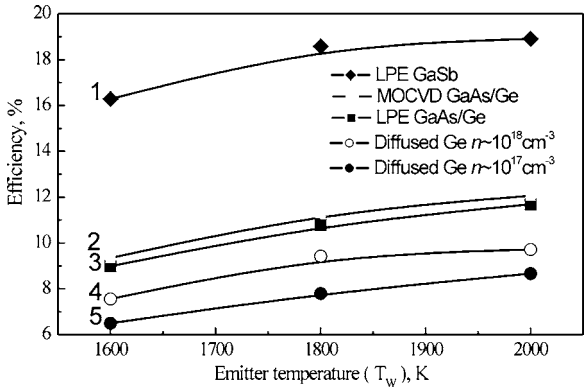

Fig. 14 Dependence of the efficiency of the TPV cells: (1) based on GaSb; (2, 3) *p*-GaAs-*p-n*-Ge structures with a wide-band window grown by LPE (curve 3) and MOCVD (curve 2); and (4, 5) based on *p-n*-Ge (bulk diffused), as a function of the tungsten emitter temperature

Figures 14 and 15 show that efficiencies in Ge cells are lower than in GaSb cells. However, the developed GaAs/Ge cells also are promising for application in solar TPV systems taking into account the lower price of Ge substrates and possibility to obtain a higher sub-band gap photon reflectance [12] for these cells in comparison with GaSb cells.

Conclusion

LPE epitaxial growth technique and zinc diffusion have been developed in application to the high efficient bottom GaSb subcells in mechanically stacked solar cells and TPV converters. Photocurrent density as high as 4.5 A/cm^2 and efficiency of 18.5% were obtained in GaSb cells illuminated by a tungsten emitter heated up to 2000 K.

The combination of the MOCVD, LPE, and Zn diffusion allows for fabricating Ge PV cells based on the GaAs/Ge heterostructure characterized by increased values of the photocurrent and the open circuit voltage. High efficiencies of 10.9% have been obtained in the Ge PV cells (AM1.5D spectrum cutoff at 1820 nm) with a GaAs window grown by MOCVD at the sunlight concentration of about 150 suns. Efficiency of 4.3% (400 suns, AM1.5D) was measured in the Ge PV cells under the GaAs top solar cells. Efficiency of 11.5% was obtained in Ge TPV cells illuminated by a tungsten emitter heated up to 2000 K.

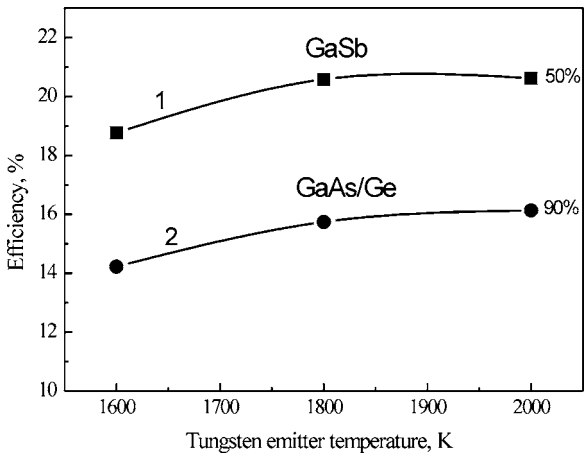

Fig. 15 The efficiency of GaSb (curve 1) and MOCVD GaAs/Ge (curve 2) based TPV cells assumed the 50% and 90% sub-bandgap photon reflection as a function of the tungsten emitter temperature

Acknowledgment

The European Commission has supported this work through funding the FULLSPECTRUM (Grant No. SES6-CT-2003-502620) project.

References

[1] Fraas, L., Avery, J. E., Martin, J., et al., 1990, "Over 35% Efficient GaAs/GaSb Tandem Solar Cells," IEEE Trans. Electron Devices, **37**(2), pp. 443–448.

[2] Andreev, V. M., Rumyantsev, V. D., Karlina, L. B., Kazantsev, A. B., Khvostikov, V. P., Shvarts, M. Z., and Sorokina, S. V., 1995, "Mechanically Stacked Concentrator Tandem Solar Cells," Proc. of the 4th European Space Power Conference, Poitiers, France, 4–8 September 1995, pp. 363–366.

[3] Bett, A. W., Dimroth, F., Stollwerck, G., and Sulima, O. V., 1999, "III-V Compounds for Solar Sell Applications," Appl. Phys. A, **A69**, pp. 119–129.

[4] Fraas, L. M., Avery, J. E., Daniels, W. E., Huang, H. X., Malfa, E., Venturino, M., Testi, G., Mascalzi, G., and Wuenning, J. G., 2002, "TPV Tube Generators for Apartment Building and Industrial Furnace Applications," AIP Conf. Proc., **653**, pp. 38–48.

[5] Andreev, V. M., Khvostikov, V. P., Rumyantsev, V. D., Gazaryan, P. Y., Vlasov, A. S., Sadchikov, N. A., Sorokina, S. V., Zadiranov, Y. M., and Shvarts, M. Z., 2005, "Thermophotovoltaic Converters With Solar Powered High Temperature Emitters," 1AP.1.2, Proc. 20th European Photovoltaic Solar Energy Conference, Barcelona, Spain, 6–10 June 2005, pp. 8–13.

[6] Stringfellow, G. B., 1974, "Calculation of Distribution Coefficients of Donors in III-V Semiconductors," J. Phys. Chem. Solids, **35**(11), pp. 775–783.

[7] Khvostikov, V. P., Rumyantsev, V. D., Khvostikova, O. A., Gazaryan, P. Y., Sorokina, S. V., Potapovich, N. S., Shvarts, M. Z., and Andreev, V. M., 2005, "Narrow Bandgap GaSb and InGaAsSb/GaSb Based Cells for Mechanically Stacked Tandems and TPV Converters," 1DO.9.6, Proc. 20th European Photovoltaic Solar Energy Conference, Barcelona, Spain, 6–10 June 2005, pp. 191–194.

[8] Luca, S., Santailler, J. L., Rothman, J., Bell, J. P., Calvat, C., Basset, G., Passero, A., Khvostikov, V. P., Potapovich, N. S., and Levin, R. V., 2007, " GaSb Crystals and Wafers for Photovoltaic Devices," ASME J. Sol. Energy Eng., **129**, pp. 304–313.

[9] Chin, V. W. L., 1995, "Electron Mobility in GaSb," Solid-State Electron., **38**(1), pp. 59–67.

[10] Caughey, D. M., and Thomas, R. E., 1967, "Carrier Mobilities in Silicon Empirically Related to Doping and Field," Proc. Inst. Electr. Eng., **55**, pp. 2192–2193.

[11] Martinm, D., and Algora, C., 2004, "Temperature-Dependent GaSb Material Parameters for Reliable Thermophotovoltaic Cell Modeling," Semicond. Sci. Technol., **19**, pp. 1040–1052.

[12] Khvostikov, V. P., Rumyantsev, V. D., Khvostikova, O. A., Shvarts, M. Z., Gazaryan, P. Y., Sorokina, S. V., Kaluzhniy, N. A., and Andreev, V. M., 2004, "Thermophotovoltaic Cells Based on Low-Bandgap Compounds," AIP Conf. Proc., **738**, pp. 436–444.

[13] Bett, A. W., Keser, S., and Sulima, O. V., 1997, "Study of Zn Diffusion into GaSb from the Vapour and Liquid Phase," J. Cryst. Growth, **181**(9), pp. 9–16.

[14] Andreev, V. M., Vlasov, A. S., Khvostikov, V. P., Khvostikova, O. A., Gazaryan, P. Y., and Sorokina, S. V., 2006, "Solar Thermophotovoltaic Converters," ASME J. Sol. Energy Eng., **129**, pp. 298–303.

[15] Boltaks, B. I., 1963, *Diffusion in Semiconductors*, Infosearch Ltd., London, U.K., Chap. VI, pp. 378.

[16] Nagashima, T., Okumura, K., Murata, K., and Yamaguchi, M., 2003, "A Germanium Back-Contact Type Cell for Thermophotovoltaic Applications," 1P-D3-10, *Proc. 3rd World Conference on Photovoltaic Energy Conversion*, Osaka, Japan, 11–18 May 2003.

[17] Bailey, S. G., Flood, D. J., Brinker, D. R., Wheeler, D. R., Alterovitz, S. A., and Scheiman, D., 1997, "Front Surface Engineering of High Efficiency Si Solar Cells and Ge TPV Cells," *Proc. 26th IEEE Photovoltaic Specialist Conference*, Anaheim, CA, 29 September–3 October 1997, pp. 847–851.

[18] Posthuma, N. E., van der Heide, J., Flamand, G., and Poormans, J., 2004, "Development of Low Cost Germanium Photovoltaic Cells for Application in TPV Using Spin on Diffusion," AIP Conf. Proc., **738**, pp. 337–344.

[19] Wojtczuk, S. J., Tobin, S. P., Sanfacon, M. M., Haven, V., Geoffroy, L. M., and Vernon, S. M., 1991, "Monolithic Two-Terminal GaAs/Ge Tandem Space Concentrator Cells," *Proc. 22nd IEEE Photovoltaic Specialists Conference*, Las Vegas, NV, 7–11 October 1991, pp. 73–79.

[20] Friedman, D. J., Olson, J. M., Ward, S., Moriarty, T., Emery, K., Kurtz, S., and Duda, A., 2000, "Ge Concentrator Cells for III-V Multijunction Devices," *Proc. 28th IEEE Photovoltaic Specialists Conference*, Anhorage, AK, 15–22 September 2000, pp. 965–967.

[21] Friedman, D. J., and Olson, J. M., 2001, "Analysis of Ge Junctions for GaInP/GaAs/Ge Three Junction Solar Cells," Prog. Photovoltaics, **9**, pp. 179–189.

[22] Andreev, V. M., Khvostikov, V. P., Kalyuzhny, N. A., Titkov, S. S., Khvostikova, O. A., and Shvarts, M. Z., 2004, "GaAs/Ge Heterostructure Photovoltaic Cells Fabricated by a Combination of MOCVD and Zinc Diffusion Techniques," J. Electron. Mater., **38**(3), pp. 355–359.